ISSN: 0975-8585

Research Journal of Pharmaceutical, Biological and Chemical Sciences

# Model and Methods for Numerical Simulation of Wave Action of Real Working Fluids in Pipelines.

**Andrei Aleksandrovich Chernousov*, Rustem Dalilovich Enikeev, and Gleb Alekseevich Nozdrin.**

Ufa State Aviation Technical University, Russian Federation, 450008, Ufa, K. Marx Street, 12.

**ABSTRACT**

The conservation laws and the equations of state for quasi-1D motion of compressible fluid in pipeline are formulated in general form, along with the conservative monotone methods suitable for real (multi-component, multiphase) working fluids. The objective is to present a concise approach to construct a general purpose model of pipeline flow for the applied software package, and to present some validation results. The known achievements on higher order monotone schemes for the hyperbolic conservation laws are applied to solve problems of flow in pipes. Specifically, characteristic-based reconstruction and approximate solution to Riemann problem in Godunov-type schemes are used to incorporate real working fluids' equations of state into explicit numerical schemes. Preliminary validation of the model and the computer code is done for equation of state of perfect gas as a special case. Shown are the solutions to problems for 2 validation cases: (a) Riemann problem (compared to the exact solution) and (b) problem of wave action (compared to the experimental data obtained on a single-cycle installation). The results encourage further generalization and testing the model to be applied to real and multiphase fluids and for compliant pipes.

**Keywords:** unsteady compressible flow, flow in pipes, one-dimensional model, numerical simulation, Godunov-type schemes, validation.

***Corresponding author***

## INTRODUCTION

Working fluids, in general case, are multi-component and multi-phase mixtures. Flow of such fluid in pipeline, in general, is an unsteady motion with the traveling waves. For accuracy and efficiency of computational simulation of such flows, corresponding models and numerical schemes must be tested and implemented into the applied software packages.

We investigate the adequacy of the model and the applicability of the chosen numerical schemes to compute unsteady flows for general industrial applications that (in principle) include complex fluid properties and fluid-structure interaction. To formulate a model of flow in pipe with a greater generality, it is needed to start with governing equations based on certain basic hypotheses. The equations (in form of conservation laws) are being closed with the sub-models of physical interactions (based on additional assumptions). The partial differential equations (PDEs) of the resulting model of the process must be solved using numerical scheme which must combine higher order of accuracy, stability and monotonicity (ensuring convergence of numerical solution to exact solution of problems). To be useful for engineering analysis, the model and the numerical scheme are to be integrated into modular software, together with other models of system components. The model, the scheme and the implementation of them both, need to be validated on real world test cases.

With a view to ameliorate applied software by applying this approach, we've implemented the model and the family of computational methods with validation using simple test cases. The governing equations of the model express the conservation laws of the quasi-1D flow in integral form (thus ensuring modeling flows with discontinuities). Closure models include the model of properties of the fluid – starting from thermal and caloric *equations of state* (EOSs), which are written in general form based on thermal and phase equilibrium hypothesis). The family of conservative monotone numerical schemes (that can be considered to be higher order Godunov-type [1] methods) is constructed based on piecewise polynomial reconstruction of characteristic variables [2] with limiter functions [2–4]. The capability of this family of methods to deal with the test problems was to be validated. To do so, we obtained and presented the solutions to (a) Riemann problem (compared with exact solution) and (b) problem of wave action (compared with the experimental data obtained on a single-cycle test installation).

### Related Work

Thus, this work is aimed at developing a model and methods for numerical simulation of wave motion of multiphase working fluids, i.e. the universal model and methods for software library for engineering analysis. This model must be, first and foremost, adequate (within the limits of its basic hypotheses) to describe wave motion of fluids with both idealized and real (and even multiphase) fluid's EOSs. At the same time, a numerical method must be of high-order accuracy and must give solutions that converge to exact solutions to the model equations in integral form.

In this regard, we have chosen conservative monotone Godunov-type methods. We considered the sub-class of these methods, which uses linearized characteristic relations for spatial reconstruction of the solution and for evaluation of fluxes at cell boundaries [1, 2, 4, 5]. At this stage, both the model and numerical methods must have been tested, including testing using experimental data (this basic theory and its validation were taken as the objective of this article).

Later the EOS of real multiphase fluids will be incorporated into the model (that seems to be rather straightforward task), as well as the sub-models of local effects that are important for real world problems – viscoelastic behavior of compliant pipes and the unsteady friction [9–11]. Each stage of generalization of the model assumes correct implementation, testing and (if necessary) calibration of the model.

### Mathematical Model

The basis of mathematical model for engineering analysis of fluid flow in pneumo- and hydromechanic systems is a system of governing equations written in rather general form. Their formulation is possible on the basis of general hypotheses – assumptions that limit the universality of the resulting model. The closure of the governing equations of non-stationary motion of the fluid by the models of specific effects in the flow provides

the model which is applicable to the real problems. This model has to be implemented by an efficient numerical scheme and then validated (and calibrated, if needed).

**Governing equations**

To formulate the governing equations, we assume (as general hypotheses) that:

– multi-component (and multi-phase) fluid, that flows within a channel (or "pipe"), can be considered as a continuous medium;
– flow is quasi-1D, i. e. the flow variables are uniformly distributed over cross-sections of the channel:

$$\boldsymbol{\psi} = \boldsymbol{\psi}(x,t) = [p, T, u, Y_1 = \rho_1 / \rho, \ldots]^T;$$

– in connection with this, we also assume that the shear stress $\tau_w = \tau_w(x,t)$ and the heat flux density $q_w = q_w(x,t)$ (both are averaged over the local perimeter) affect the fluid element in a cross section instantly, as well as the normal stress, which is equal to the thermodynamic pressure $p = p(x,t)$;

– thermodynamic and phase equilibrium holds locally (i.e., for each particle of such fluid), so that the flow variables (other than velocity $u$) are interrelated by EOSs;

– transfer in the longitudinal direction is determined by convection and by transfer of momentum and energy due to the pressure.

As the consequences of all these assumptions, a system of conservation laws can be written using symbolic "vector" notation:

$$\frac{d}{dt}\int_{x_1}^{x_1+\Delta x} \mathbf{U} F dx = -(\mathbf{F}_x F)\Big|_{x_1}^{x_1+\Delta x} + \int_{x_1}^{x_1+\Delta x} \mathbf{S} F dx, \qquad (1)$$

where $\mathbf{U} = [\rho_1, \ldots, \rho_K, \rho u, \rho E]^T$ is the vector of conservative variables, $\mathbf{F}_x = [\rho_1 u, \ldots, \rho_K u, \rho u^2 + p, \rho u E + p u]^T$ is the flux vector, $\mathbf{S} = [0, \ldots, 0, \tau_w \Pi / F + p(dF/dx), q_w \Pi / F]^T$ is the vector of sources, $E = e + u^2/2$ is the specific total energy, $\tau_w$ is the shear stress and $q_w$ is the heat flux density (averaged over the perimeter of the cross section). For noncompliant pipes (the only case considered here), perimeter $\Pi$ and cross-sectional area $F$ are pre-defined smooth (differentiable) functions of $x$.

There also must be a one-to-one conversion $\mathbf{U}$ to $\mathbf{p}$, where $\mathbf{p}$ is the vector of "primitive" variables used in the formulation of the problem (for initial and boundary conditions) and for presenting its solution; in this paper

$$\mathbf{p} = [p, T, u, Y_1, \ldots, Y_K]^T. \qquad (2)$$

**Closure models**

Governing equations (1) express the conditions of conservation of masses of individual mixture constituents, the momentum and the energy of the mixture. A closed system of equations of a specific model will be based on conservation laws (1) and will contain equations of specific sub-models.

First, it is necessary to provide the particular *equations of state* (EOSs) of the multi-component fluid, corresponding to the general forms:

$$p = p(\rho, T, Y_1, \ldots, Y_K) = p(\rho, T, \mathbf{Y}), \qquad (3)$$
$$e = e(\rho, T, Y_1, \ldots, Y_K) = e(\rho, T, \mathbf{Y}). \qquad (4)$$

The remaining unknowns in (1): $\tau_w$ and $q_w$, must be expressed using other dependent variables, i. e., $\tau_w = \tau_w(x,t) = \tau_w(\mathbf{p}(x,t),t)$ and $q_w = q_w(x,t) = q_w(\mathbf{p}(x,t),t)$. Models of friction and heat transfer can be either empirical or semi-empirical and ultimately must be calibrated under steady flow conditions. Specific equations of these models (as well as the EOSs) are shown below (see Validation section).

**Numerical methods**

To construct a numerical method that approximates (1) on a mesh of finite volume cells, we define $\mathbf{U}_i^n$ as the volume averaged values of the conservative variables for $i$-th cell at $t = t^n$:

$$\mathbf{U}_i^n = \frac{(\mathbf{U}F)_i^n \cdot \Delta x}{F_i^n \cdot \Delta x}, \ (\mathbf{U}F)_i^n \cdot \Delta x = \\ = \int_{x_{i-1/2}}^{x_{i+1/2}} \mathbf{U}F dx, \ V_i^n = F_i^n \cdot \Delta x = \int_{x_{i-1/2}}^{x_{i+1/2}} F dx, \tag{5}$$

$(\mathbf{F}_x F)_{i-1/2}^n$ as the flux of $(\mathbf{U}F)_i^n \cdot \Delta x$ at the cell boundary (i. e., at $x = x_{i-1/2}$), and $(\mathbf{S}F)_i^n \cdot \Delta x$ as its instantaneous source.

Then the spatial approximation of (1) at $t = t^n$ takes the form:

$$\left(\frac{d\mathbf{U}}{dt}\right)_i^n \approx \frac{1}{F_i}\left[\frac{(\mathbf{F}_x F)_{i-1/2}^n - (\mathbf{F}_x F)_{i+1/2}^n}{\Delta x} + (\mathbf{S}F)_i^n\right] = \\ = \mathbf{L}(\{\mathbf{U}\}_i^n, t^n, \Delta x, \ldots) = \mathbf{L}_i^n. \tag{6}$$

The order of accuracy of differential operator $\mathbf{L}_i^n$ in (6) is defined by adopted spatial reconstructions $F(x)$, $\mathbf{U}_i^n(x)$, $(\mathbf{F}_x)_i^n(x)$ и $\mathbf{S}_i^n(x)$. So curly braces in the definition of $\mathbf{L}_i^n$ denote the values of $\mathbf{U}_i^n$ in the cells of certain stencil.

**Runge – Kutta integration with respect to time**

In order to approximate (1) with respect to time, we use the family of Runge – Kutta methods (thus applying method of lines to $i$ th cell).

The Euler method of updating the dependent variables in the cell can be written in this notation as

$$\mathbf{U}_i^{n+1} = \mathbf{U}_i^n + \Delta t \cdot \mathbf{L}_i^n, \tag{7}$$

the modified Euler method (second order method with two stages) as

$$\mathbf{U}_i^{(1)} = \mathbf{U}_i^n + \Delta t \cdot \mathbf{L}_i^n, \tag{8}$$

$$\mathbf{U}_i^{n+1} = \tfrac{1}{2}\mathbf{U}_i^n + \tfrac{1}{2}\mathbf{U}_i^{(1)} + \tfrac{1}{2}\Delta t \cdot \mathbf{L}_i^{(1)}, \tag{9}$$

and the three-stage, third order "low storage" method (recommended in [4]) as

$$\mathbf{U}_i^{(1)} = \mathbf{U}_i^n + \Delta t \cdot \mathbf{L}_i^n, \tag{11}$$

$$\mathbf{U}_i^{(2)} = \tfrac{3}{4}\mathbf{U}_i^n + \tfrac{1}{4}\mathbf{U}_i^{(1)} + \tfrac{1}{4}\Delta t \cdot \mathbf{L}_i^{(1)}, \tag{12}$$

$$\mathbf{U}_i^{n+1} = \tfrac{1}{3}\mathbf{U}_i^n + \tfrac{2}{3}\mathbf{U}_i^{(2)} + \tfrac{2}{3}\Delta t \cdot \mathbf{L}_i^{(2)}. \tag{13}$$

At each stage of each method, the updated primary variables (2) must be calculated from the updated conservative variables for the cells. For example, at final stages of all these methods, the calculation of $\mathbf{p}_i^{n+1}$ starts by "decoding" the updated "vector" $\mathbf{U}_i^{n+1}$:

$$\rho_i^{n+1} = \sum_k (\rho_k)_i^{n+1},\ (Y_k)_i^{n+1} = (\rho_k)_i^{n+1} / \rho_i^{n+1},\ u_i^{n+1} = (\rho u)_i^{n+1} / \rho_i^{n+1},$$

$$e_i^{n+1} = (\rho E)_i^{n+1} / \rho_i^{n+1} - (u_i^{n+1})^2 / 2,$$

the temperature is calculated either explicitly from the caloric EOS (4): $T_i^{n+1} = T(\rho_i^{n+1}, e_i^{n+1}, \mathbf{Y}_i^{n+1})$, or is obtained as a root $T_i^{n+1}$ of (4) $e_i^{n+1} = e(\rho_i^{n+1}, T_i^{n+1}, \mathbf{Y}_i^{n+1})$ by iterations. Finally, the pressure is calculated from the thermal EOS (3): $p_i^{n+1} = p(\rho_i^{n+1}, T_i^{n+1}, \mathbf{Y}_i^{n+1})$, where $\mathbf{Y}_i^{n+1} = [(Y_1)_i^{n+1}, ..., (Y_K)_i^{n+1}]^T$ is a "vector" of mass fractions.

**Piecewise-polynomial reconstruction**

To approximate fluxes with respect to $x$, we use the piecewise-polynomial reconstruction of the dependent variables. Piecewise-constant, linear and parabolic reconstructions are used for the methods (7), (8)–(9) and (11)–(13), respectively. As proposed in [2], the dependent variables used in these reconstructions may be the invariants of the linearized system of equations in characteristic form deduced from (1). Thus, passing to the limit as $\Delta x \to dx \to 0$, the governing equations (1) can be (in sub-domains without discontinuities) converted to an equivalent system of *partial differential equations* (PDEs):

$$\frac{\partial \mathbf{U}F}{\partial t} + \frac{\partial \mathbf{F}_x F}{\partial x} = \mathbf{S}F,$$

which can be, in turn, converted to an equivalent characteristic form (with account for the equations of state in the general form) [6]. Further, for our purpose, the terms in the right-hand sides of the first three equations of the obtained system of PDEs (i. e., terms accounting of variations of composition and of the channel profile, of friction and heat transfer to the walls) can be discarded, and the equations can be linearized. This yields:

$$\frac{\partial \mathbf{I}}{\partial t} + \mathbf{c}\frac{\partial \mathbf{I}}{\partial x} = 0, \qquad (14)$$

where $\mathbf{c} = [u + c, u - c, c, u, ..., u]^T$ are the characteristic speeds, and $\mathbf{I} = [I_+, I_-, I_0, Y_1, ..., Y_K]^T$, where

$$I_\pm = u + \alpha_\pm p,\ \alpha_\pm = \pm\frac{1}{\rho c},\ I_0 = p + \alpha_0 \rho,\ \alpha_0 = -c^2, \qquad (15)$$

and all $\mathbf{I}$ components (provided that $\alpha_+,\ \alpha_-,\ \alpha_0$ are constants) are the invariants of the system (14) that stay unchanged along the respective "characteristic" directions in в $(x, t)$. Equations (14) describe the motion of the fluid in the "acoustic" approximation, i. e., for small deviations of state variables $\rho,\ c, ...$ from constants ($\rho_0,\ c_0, ...$). However, the flux evaluation procedures at the cell boundaries based on (14) can be applied [2] to problems with nonlinear governing equations (1).

We used (in general) piecewise-parabolic reconstructions of $\mathbf{I}$ components within each cell:

$$\begin{aligned}\mathbf{I}_i^n(x) = \mathbf{I}_i^n + \frac{\tilde{\Delta}\mathbf{I}_i^n + \tilde{\nabla}\mathbf{I}_i^n}{2\Delta x}(x - x_i) + \\ + \varphi\frac{\tilde{\Delta}\mathbf{I}_i^n - \tilde{\nabla}\mathbf{I}_i^n}{\Delta x^2}(x - x_i)^2,\ x_{i-1/2} < x < x_{i+1/2},\end{aligned} \qquad (16)$$

$$\tilde{\Delta}\mathbf{I}_i^n = \text{minmod}(\,\Delta\mathbf{I}_i^n, b\nabla\mathbf{I}_i^n),\ \ \tilde{\nabla}\mathbf{I}_i^n = \text{minmod}(\,\nabla\mathbf{I}_i^n, b\Delta\mathbf{I}_i^n),$$

$$\Delta\mathbf{I}_i^n = \mathbf{I}_{i+1}^n - \mathbf{I}_i^n,\ \ \nabla\mathbf{I}_i^n = \mathbf{I}_i^n - \mathbf{I}_{i-1}^n,\ \ \mathbf{I}_i^n = \mathbf{I}(\mathbf{U}_i^n),$$

where $1 \le b \le b_{\max} = (3-\varphi)/(1-\varphi),\ \ \varphi \le 1,$ and the monotonicity preserving limiter function [4]:

$$\text{minmod}(\,y, z) = \frac{\text{sign}(y) + \text{sign}(y)}{2} \cdot \min(|\,y\,|, |\,z\,|).$$

According to (16), components of $\mathbf{I}$ found on the left and right sides of a cell boundary (for example, at the first stage of each method – $\mathbf{I}_{i+1/2,\,L}^n$ and $\mathbf{I}_{i+1/2,\,R}^n$) are determined [3] as

$$\mathbf{I}_{i+1/2,\,L}^n = \mathbf{I}_i^n + \frac{1+\varphi}{4}\tilde{\Delta}\mathbf{I}_i^n + \frac{1-\varphi}{4}\tilde{\nabla}\mathbf{I}_i^n, \tag{17}$$

$$\mathbf{I}_{i+1/2,\,R}^n = \mathbf{I}_i^n + \frac{1+\varphi}{4}\tilde{\Delta}\mathbf{I}_i^n + \frac{1-\varphi}{4}\tilde{\nabla}\mathbf{I}_i^n. \tag{18}$$

The piecewise-parabolic reconstruction (16) with $b = b_{\max}$ and $\varphi = 1/3$ was applied for the method (11)–(13), the piecewise-linear reconstruction ($b = \varphi = 1$) for the method (8)–(9), and the piecewise-constant reconstruction ($\tilde{\Delta}\mathbf{I}_i^n = \tilde{\nabla}\mathbf{I}_i^n = 0$) for (7). With these settings, the methods provide, respectively, the third, second and first order of accuracy [3] when applied to smooth solutions of a "model" hyperbolic equation, for example, $\partial u/\partial t + \partial u/\partial x = 0.$

**Approximate Riemann solver**

Fluxes in the described methods are calculated from approximate solution of the Riemann problem at the boundary between two cells. Here, the initial data of the problem are the calculated from (17) and (18) invariants of the system (14). Thus, at the first stage of each method:

$$(\mathbf{F}_x)_{i+1/2}^n = \mathbf{F}_x(\mathbf{p}_{i+1/2}^n),\ \ \mathbf{p}_{i+1/2}^n = \mathbf{p}(\mathbf{I}_{i+1/2,\,L}^n, \mathbf{I}_{i+1/2,\,R}^n).$$

The dependent variables at the boundary (for example, at the first stages of methods) are defined by (15), as proposed in [2]:

$$\begin{aligned} &p_{i+1/2}^n = \frac{I_+ - I_-}{\alpha_+ - \alpha_-},\ \ \rho_{i+1/2}^n = \frac{I_0 - p_{i+1/2}^n}{\alpha_0}, \\ &T_{i+1/2}^n = T(\rho_{i+1/2}^n, p_{i+1/2}^n, \mathbf{Y}),\ \ u_{i+1/2}^n = I_+ - \alpha_+ p_{i+1/2}^n, \end{aligned} \tag{19}$$

where e. g. for the flow to the right at a subsonic speed (i. e., when $u_{i+1/2}^n \ge 0,\ u_{i+1/2}^n + c_{i+1/2}^n \ge 0$ and $u_{i+1/2}^n - c_{i+1/2}^n < 0$)

$$I_+ = (I_+)_{i+1/2,\,L}^n,\ \ I_- = (I_-)_{i+1/2,\,R}^n,\ \ I_0 = (I_0)_{i+1/2,\,L}^n,\ \ \mathbf{Y} = \mathbf{Y}_{i+1/2,\,L}^n,$$

where $\alpha_+$, $\alpha_-$ и $\alpha_0$ are assumed (as well as $\mathbf{I}$) to be constant along the respective characteristics [2]. For the special case of perfect gas (with $R = \text{const}_1$ и $\gamma = c_p / c_V = \text{const}_2$, as in our simulations below), simple conversion $[\alpha_+, \alpha_-, \alpha_0]^T = \mathbf{a}(\mathbf{I})$ is possible:

$$\alpha_\pm = \mp\frac{\gamma-1}{2} \cdot \frac{I_+ - I_-}{I_0},\ \ \alpha_0 = -\,[c = \frac{\gamma}{2}(I_+ - I_-)]^2.$$

Note that the described above calculation can be implemented iteratively, but we used it in a simplest fashion, with the following simplistic initial guess for the velocity and the speed of sound at the cell boundary:

$$u_{i+1/2}^{n,(1)} = \frac{1}{2}\left[\frac{(I_+)_{i+1/2,L}^n + (I_-)_{i+1/2,L}^n}{2} + \frac{(I_+)_{i+1/2,R}^n + (I_-)_{i+1/2,R}^n}{2}\right],$$

$$c_{i+1/2}^{n(1)} = \frac{\gamma}{2}\left[\frac{(I_+)_{i+1/2,L}^n - (I_-)_{i+1/2,L}^n}{2} + \frac{(I_+)_{i+1/2,R}^n - (I_-)_{i+1/2,R}^n}{2}\right].$$

After this, components of $\mathbf{p}_{i+1/2}^n$ are calculated according to (19), $e_{i+1/2}^n = e(\rho_{i+1/2}^n, p_{i+1/2}^n, \mathbf{Y}_{i+1/2}^n)$ is evaluated by (4), and finally the flux "vector" in (6) is evaluated as

$$(\mathbf{F}_x F)_{i+1/2}^n = \mathbf{F}_x(\mathbf{I}_{i+1/2,L}^n, \mathbf{I}_{i+1/2,R}^n)\cdot F = \mathbf{F}_x(\mathbf{p}_{i+1/2}^n)\cdot F =$$
$$= [(GY_1)_{i+1/2}^n, ..., (GY_1)_{i+1/2}^n, (Gu + pF)_{i+1/2}^n, (Gh^*)_{i+1/2}^n]^T,$$

where $G = \rho u F$ is the mass flow rate of the fluid and $h^* = e + p/\rho + u^2/2 = h + u^2/2$ is its specific total enthalpy.

**Validation**

To validate the model and its numerical implementation, we solved the following two test problems.

The first test case is the Riemann problem, which has a well known exact solution.

The second test is a series of simulations of unsteady motion of air in a special installation, compared with experiments. For both cases, a model of the perfect gas was used for EOSs of the compressible fluid: $p = \rho RT$ and $e = c_V T$ with constant parameters $R = 287{,}1$ J/(kg · K) and $\gamma = (c_p = c_V + R)/c_V = 1{,}4$ that corresponds to the air. With such EOSs, the mass fraction $Y_1$ of the 1st constituent of the mixture can be considered as a "passive scalar".

**Riemann problem**

The Riemann problem was chosen for the first test case, in which the following parameter vectors were set as initial conditions in semi-spaces to the left (L) and to the right (R) from $x_{\max} = 50$ m:

$$p_L = 200\text{ kPa};\ p_R = 100\text{ kPa};\ T_L = T_R = 300\text{ K};$$
$$u_L = u_R = 0;\ (Y_1)_L = 0.1;\ (Y_1)_R = 0.8.$$

The model (1) with $F = 0$, $\tau_w = 0$ and $q_w = 0$ was used, which allowed to describe the "self-similar" flow pattern with the centered rarefaction wave, contact discontinuity and shock wave.

Computational mesh contained 100 equally sized cells ($\Delta x = 1.0$ m), $N = 180$ time steps with $\Delta t$ corresponding to the Courant number of 0.25. Numerical solutions to the test problem were obtained by three methods of various orders of accuracy in time (11)–(13) and reconstructions in $x$ of corresponding orders of accuracy. The numerical solutions $p_i^N$, $T_i^N$, $u_i^N$ and $(Y_1)_i^N$ (for $t^N = N\cdot\Delta t$) and the exact solution are plotted in Fig. 1.

This test has shown the almost complete absence of oscillations at discontinuities in solutions obtained by all three methods. Also it is shown a substantial reduction of the numerical diffusion with an increase in the formal order of accuracy of the method (as it is usually the case for the methods of this class).

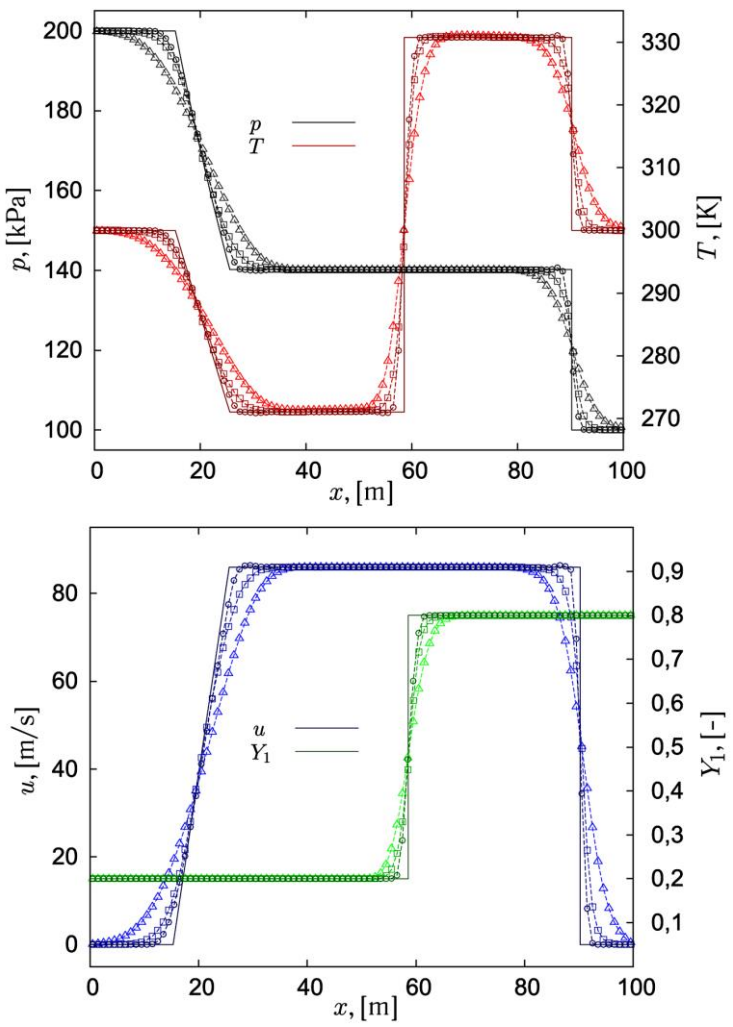


**Fig.1. Numerical solutions to the Riemann problem (by methods of the 1st, 2nd and 3rd order of accuracy) compared with the exact solution.**

**Waves traveling in a pipeline**

By testing the model and the numerical methods on the gas dynamics problem with known exact solution, we proved merely the correctness of a software implementation of the "core" of the model. Further, the model was to be tested by simulating the wave action in a pipeline with friction and heat transfer to the walls.

We used the measurements of rapidly varying pressure obtained on the pipeline with finite-amplitude waves in the air as a working fluid.

The general view of the experimental installation [7] with the wave generator is shown in Fig. 2, a, and the pipeline schematic views with sensors (two variants of setup) is shown in Fig. 2, b and c.

The lengths of the individual pipes (see Fig. 2, b and c) are $l_1 = 3028$ mm and $l_2 = 3692$ mm; their diameters: $d_1 = 24{,}1$ mm and $d_2 = 24{,}4$ mm, coordinates of the sensors: $l_{p1} = 781$ mm and $l_{p2} = 922$ mm; volume of the plenum: $V = 748{,}2$ cm$^3$; the parameters of the environment (air in the laboratory) are $p_0 = 100{,}26$ kPa и $T_0 = 299{,}3$ K.

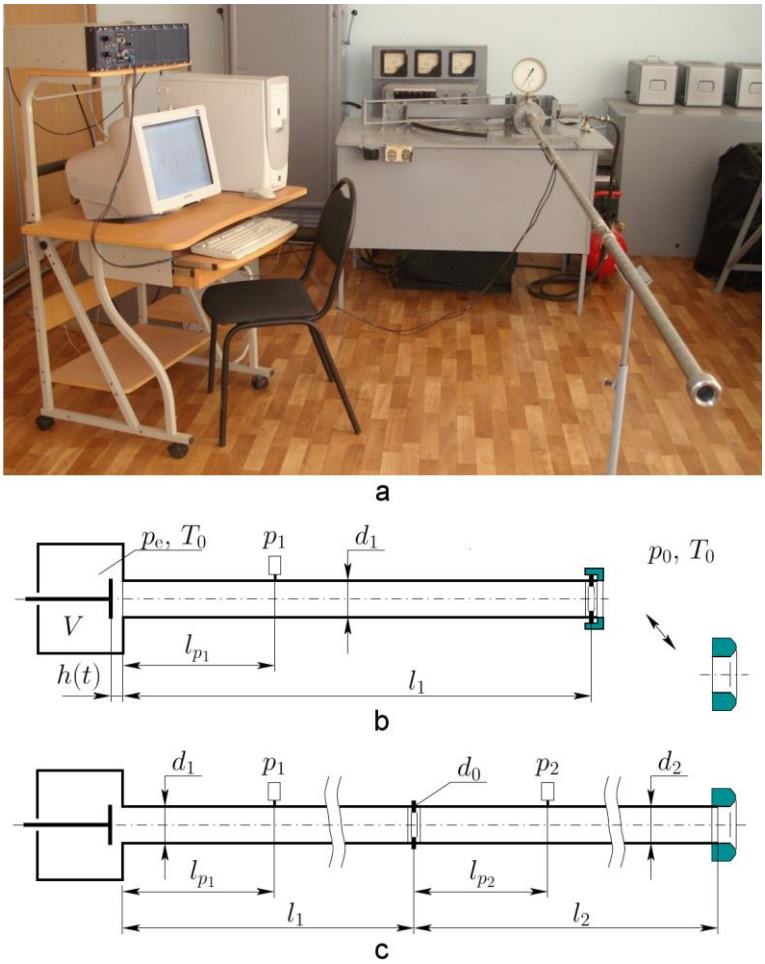


**Fig.2. The installation (a) view; (b) and (c): two variants of its pipeline and sensors setup.**

The model (1) used here assumed $F = \text{const}$ for each individual pipe, and $\tau_w$ и $q_w$ were determined by the models valid for the steady flow: the shear stress was expressed as:

$$\tau_w = -\lambda \cdot \frac{\rho |u| u}{2 d_{eff}} \cdot \frac{F}{\Pi},$$

where $1/\sqrt{\lambda} = 2\log_{10}(\mathrm{Re}\sqrt{\lambda}) + 0{,}8$, and the local heat flux density was determined using the Reynolds analogy:

$$q_w = \lambda \cdot \frac{\rho |u|}{2 d_{eff}} \cdot \frac{F}{\Pi} \cdot c_p (T_w - T^*), \text{where} T^* = T + \frac{u^2}{2 c_p}.$$

In addition to the model of flow within the channel, rather basic models of the plenum and of the flow through the flow restriction were used.

Models of flow restrictions and their incorporation into numerical scheme are described in [8].

Total pressure losses (on steel diaphragms of various diameters $d_0$ and on "Bernoulli lemniscate", see. Fig. 2, b and c) were specified by the characteristics in the forms $p^*_{\text{out}} / p^*_{\text{in}} = \sigma(M_{\text{in}})$ and $p^*_{\text{out}} / p^*_{\text{in}} = \sigma(M_{\text{out}})$, which have been obtained by blow down under stationary flow conditions. Characteristic of losses in air flow into the plenum through a poppet valve was specified in the form $p_{\text{e}} / p^*_{\text{in}} = \sigma(M_{\text{in}}, h)$,

based on the results of 2D CFD simulation. "Laws" of the valve lift $h(t)$ were specified after optimizing the free parameters of $h(t)$ in terms of best fit of the computed and the measured pressure profiles in initial rarefaction wave.

Calculations were carried out by three-stage higher order method (11)–(13), with cell sizes of $\Delta x = 15$ mm and a time step of $\Delta t = 10^{-5}$ s (so that mesh is fine enough to eliminate effect of these parameters on the numerical solution). Calculated and measured pressures on the sensors are shown in Fig. 3 (for 2 experiments corresponding to installation setup shown in Fig. 2, b) and in Fig. 4 are for the setup shown in Fig. 2, c.

From the graphs in Fig. 3 and 4, one can see that qualitatively all the wave patterns are reproduced well by the model. The marked quantitative difference is observed mainly in the speed of the waves (calculated speed is overstated by 2-2.5%). This “effect” is well known in unsteady flows of water and gas and is attributed to the unsteady nature of friction phenomena [9, 10].

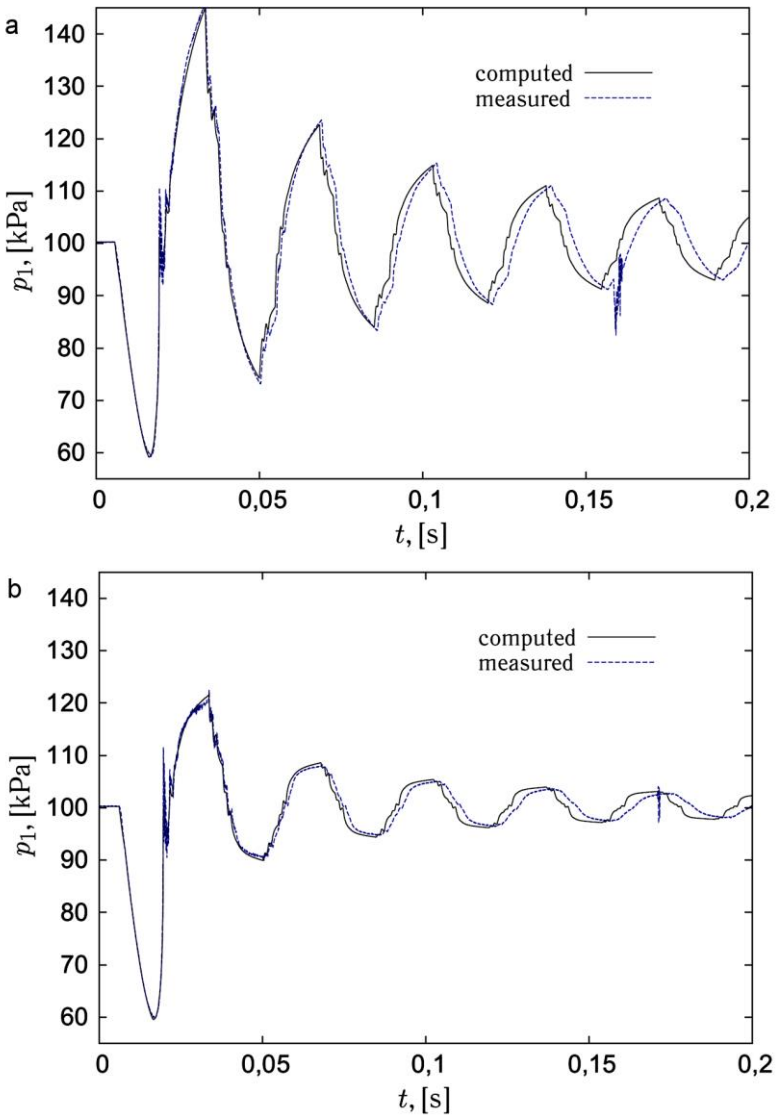


**Fig.3. Computed vs. measured $p_1(t)$ on the pressure sensor (Fig. 2, b): (a) "Bernoulli lemniscate" and (b) $d_0 = 18$ mm at the end of the pipe**

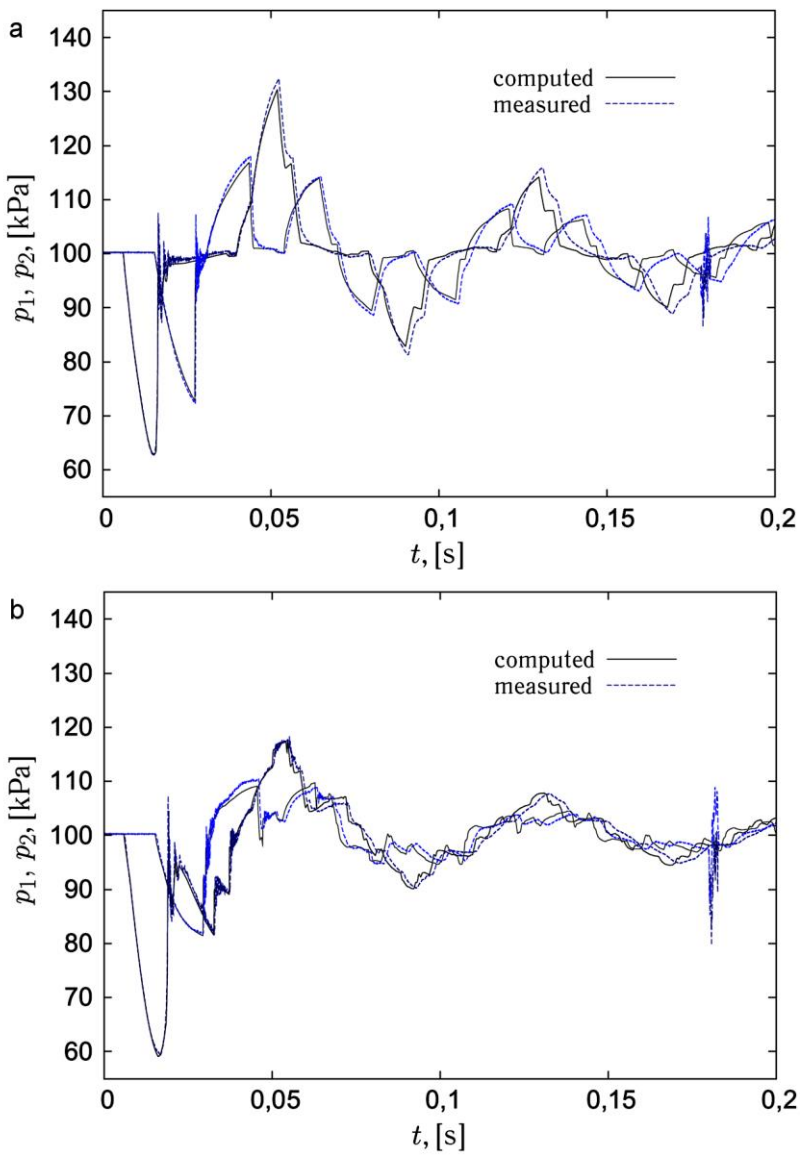


**Fig.4. Computed vs. measured $p_1(t)$ and $p_2(t)$ (see. Fig. 2, c): (a) no diaphragm and (b) diaphragm with $d_0 = 14$ mm (between the pipes)**

## CONCLUSION

This model and the numerical methods tested are already included into the applied model library for engineering analysis.

Generalization and further testing of the model and the methods are needed to account for effects of unsteady friction, viscoelastic pipe wall compliance and local flow restrictions. The models of significant local effects must be represented (along with the adequate EOS for real multiphase fluid) within the general system of conservation laws, and must be solved with the higher order monotone method.

The results obtained to date by other researchers [9–11] encourage incorporation sub-models of such effects into the model and further testing it as well as the class of numerical methods used.

## ACKNOWLEDGEMENTS

The authors acknowledge receiving support from basic part of state-funded research program of the Ministry of Education and Science of the Russian Federation for the years 2014-2016.

## REFERENCES


[1] Godunov, S.K, 1959. A difference method for numerical calculation of discontinuous solutions of the equations of hydrodynamics. Matematicheskii Sbornik, 47(3): 271-306. (In Russian).

[2] Kopchenov, V.I. and A.N. Kraiko, 1983. A monotonic second-order difference scheme for hyperbolic systems with two independent variables. USSR Computational Mathematics and Mathematical Physics, 23(4): 50-56.

[3] Ivanov, M.Ya., V.G. Krupa and R.Z. Nigmatullin, 1989. A high-accuracy version of Godunov's implicit scheme for integrating the Navier-Stokes equations. USSR Computational Mathematics and Mathematical Physics, 29(3): 170-179.

[4] Gottlieb, S. and C.-W. Shu, 1998. Total variation diminishing Runge-Kutta schemes. Mathematics of Computations, 67: 73-85.

[5] Gilmanov, A.N., 2000. A Local Characteristic Approach in High-Order Differencing. Computational Mathematics and Mathematical Physics, 40(4): 529-533.

[6] Rozdestvenskii, B.L. and N.N. Yanenko, 1983. Systems of quasilinear equations and their applications to gas dynamics. Providence: Amer. Math. Society, pp: 676.

[7] Grishin, Yu.A. and B.P. Rudoi, 1976. Installation for the generation of finite amplitude waves. Elementi teorii i rascheta rabochikh processov DVS, 1: 53-55. (In Russian).

[8] Chernousov, A.A., 2007. Conservative characteristic-based scheme for the simulation of non-stationary flows in pipelines. Voprosi teorii i rascheta rabochikh processov teplovykh dvigatelei, 21: 246-254. (In Russian).

[9] Adamkowski, A. and M. Lewandowski, 2006. Experimental Examination of Unsteady Friction Models for Transient Pipe Flow Simulation. Journal of Fluids Engineering, 128(6): 1351-1363.

[10] Kim, Y.I., 2008. Advanced Numerical and Experimental Transient Modeling of Water and Gas Pipeline Flows Incorporating Distributed and Local Effects, Ph. D. thesis, The University of Adelaide, Australia.

[11] Bousso, S. and M. Fuamba, 2013. Numerical Simulation of Unsteady Friction in Transient Two-Phase Flow with Godunov Method. Journal of Water Resource and Protection, 5(11): 1048-1058.